EUROPHYSICS LETTERS 15 July 2004

Europhys. Lett., **67** (2), pp. 240–246 (2004)
DOI: 10.1209/epl/i2004-10052-6

Layer-dependent band dispersion and correlations using tunable soft X-ray ARPES

N. Kamakura[1], Y. Takata[1], T. Tokushima[1], Y. Harada[1], A. Chainani[1,2], K. Kobayashi[3] and S. Shin[1,4]

[1] *RIKEN, Harima Institute - 1-1-1 Kouto, Mikazuki, Sayo, Hyogo 679-5148, Japan*
[2] *Institute for Plasma Research - Bhat, Gandhinagar 382 428, Gujarat, India*
[3] *SPring-8/JASRI - Mikazuki, Hyogo 679-5198, Japan*
[4] *Institute for Solid State Physics, University of Tokyo Kashiwanoha, Kashiwa, Chiba 277-8581, Japan*

(received 22 January 2004; accepted in final form 3 May 2004)

PACS. 71.20.Be – Transition metals and alloys.
PACS. 79.60.-i – Photoemission and photoelectron spectra.
PACS. 75.50.Cc – Other ferromagnetic metals and alloys.

Abstract. – Soft X-ray Angle-Resolved Photoemission Spectroscopy is applied to study in-plane band dispersions of nickel as a function of probing depth. Photon energies between $h\nu = 190$ and 780 eV were used to effectively probe up to $\sim$ 3–7 layers ($\sim$ 5–12 Å). The results show layer-dependent band dispersion of the $\Delta_{2\downarrow}$ minority spin band which crosses the Fermi level in 3 or more layers, in contrast to the known top 1-2 layers dispersion obtained using ultra-violet rays. The layer dependence corresponds to an increased value of exchange splitting and suggests reduced-correlation effects in the bulk compared to the surface.

Introduction. – Angle-Resolved Photoemission Spectroscopy (ARPES) is a valuable tool to study the experimental band structure (BS), $w(\boldsymbol{k})$, where w is the energy and $\boldsymbol{k}$ is the momentum of electrons in a solid. Recent ultra-violet ARPES (ARUPS) studies of correlated materials have provided important results like spin and charge collective modes in a quasi-1D (dimensional) metal [1], dimensional crossover [2], exotic characteristics of the high-T_c cuprates [3], etc. While ARUPS is extremely well suited to study the electronic BS of low-dimensional solids, it probes the top 1-2 layers of the surface [4]. In order to determine the bulk BS of 3D correlated systems which can depend on the probed layer [5–8], it is meaningful to use higher energies. As the excitation energy is increased, the probing depth or mean free path (MFP) increases [9], but, to date, no layer-dependent variation of the in-plane band dispersion (BD) beyond the top 2 layers has been reported. In this work, using tunable soft X-ray ARPES, we study the layer dependence of in-plane BDs of nickel metal.

Nickel is a prototype of a correlated ferromagnetic metal and has been extensively studied using PES and inverse-PES [10–19]. Beginning with the work of Slater [20] and Stoner [21], the BS of nickel has remained a suitable testing ground for a variety of experiments and theory. Recent theories have addressed the major inconsistencies with experiment: $3d$ bandwidth

extent, temperature (T) dependence of magnetization, and a satellite structure which appears at about 6 eV below the Fermi level ($E_{\rm F}$). The $3d$ bandwidth and exchange splitting (ES) of nickel observed by ARUPS are reduced by 25% and 50%, respectively [10–15], compared to the values obtained from spin-polarized local density approximation (s-LDA) calculations [22]. The 6 eV satellite obtained in PES experiments [16–18] is the two-hole bound state due to correlation effects. It is missing in BS calculations in the one-electron picture [22] but obtained in "generalized Hubbard models" [14,19,23] or the "LDA (GWA)+DMFT" (Dynamical Mean-Field Theory) [24,25] which explicitly include Coulomb interactions. A recent study discusses the inability of s-LDA to reproduce the position of the minority spin state $X_{2\downarrow}$ below $E_{\rm F}$ obtained by ARUPS [14]. The energy position of $X_{2\downarrow}$ states determines the electron count associated with the hole pocket of minority spin character at the X-point, which in turn influences the magnetic moment, a macroscopic property. Although recent theoretical efforts reproduce the experimental BS of nickel by including correlation effects [14, 25], the results were compared with experimental BS obtained using ARUPS. The present study reports new experimental results of the bulk BS of nickel obtained using soft X-ray ARPES.

Experiment. – Experiments were performed at beam line 27SU of SPring-8 [26] using linearly polarized light. Total energy resolution was 50–160 meV. The beam line has a figure-8 undulator [27], enabling an easy switch of the polarization vector from horizontal (H) to vertical (V) polarization. Ni(100) surface was prepared by Ar^+ sputtering and annealing. The surface was checked by core level photoemission spectra obtained using 780 eV photons and the contamination due to oxygen and carbon was measured to be $< 1\%$. The surface crystallinity was confirmed to be a sharp (1×1) LEED pattern.

ARPES measures w and $\boldsymbol{k}$ of electrons in a solid according to the following equations [4]:

$$\hbar \boldsymbol{k}_{\parallel} = \sqrt{2m(h\nu - w - \phi)} \sin\theta_{\rm e}\,, \tag{1}$$

$$\hbar \boldsymbol{k}_{\perp} = \sqrt{2m\{(h\nu - w - \phi)\cos^2\theta_{\rm e} + V_0\}}\,, \tag{2}$$

where $\boldsymbol{k}_{\parallel}$ and $\boldsymbol{k}_{\perp}$ are the parallel and perpendicular components of $\boldsymbol{k}$, respectively, $\theta_{\rm e}$ is the electron emission angle, ϕ is the work function, and V_0 is the inner potential. The angular resolution of the electron energy analyzer was better than $\pm 0.2^\circ$, which corresponds to resolutions of about ± 0.014, ± 0.021, and ± 0.028 $(2\pi/a_{\rm Ni})$ in $\boldsymbol{k}_{\parallel}$ at $h\nu = 190$, 435, and 780 eV, respectively (eq. (1)). Equations (1) and (2) indicate that when ARPES with fixed $h\nu$ is used for the measurement of in-plane ($\boldsymbol{k}_{\parallel}$) BDs, $\boldsymbol{k}_{\perp}$ also changes. The variation of $\boldsymbol{k}_{\perp}$ can be substantial in ARUPS [28], but diminishes with increasing $h\nu$, making it an advantage. In fig. 1(a), we plot $\boldsymbol{k}_{\perp}$ *vs.* $\boldsymbol{k}_{\parallel}$ in units of $(2\pi/a_{\rm Ni})$ for $h\nu = 190$, 435, and 780 eV in the experimental geometry of fig. 1(b), using eqs. (1) and (2) with $V_0 = 9.3$ eV. Actually, the momentum transfer of the photon is not negligible in soft X-ray ARPES. However, since our experimental geometry is near grazing incidence (fig. 1(b)), the momentum transfer of the photon results in a constant shift of the parallel component of the momentum $\boldsymbol{k}_{\parallel}$, and $\boldsymbol{k}_{\perp}$ is negligibly influenced [29]. Therefore, from fig. 1(a) the spectra of $\boldsymbol{k}_{\parallel} = 0$ at these $h\nu$ (190, 435, and 780 eV) are expected to probe an equivalent $\boldsymbol{k}_{\perp}$-point (Γ) in the 3D Brillouin zone (BZ) of Ni(100) (fig. 1(c)). We first validate this by $h\nu$-dependent ARPES of $\boldsymbol{k}_{\parallel} = 0$ in successive BZs (figs. 1(d) and (e)). (The spectra of $\boldsymbol{k}_{\parallel} = 0$ are identified from the observed band dispersion in the ($\theta_{\rm e}$-dependent) ARPES at each photon energy.) The changes in peak positions correspond to $\boldsymbol{k}_{\perp}$ BD, mainly due to the Δ_1 band. The similarity of spectra in figs. 1(d) and (e) measured in successive BZs confirm we are at equivalent momentum regions and the Γ-point can be precisely measured according to eq. (2) even by soft X-ray ARPES. Further, since the difference of $\boldsymbol{k}_{\perp}$ along Γ-X (Δ-line) of $\boldsymbol{k}_{\parallel}$ is already small with 190 eV photons (fig. 1(a)), the in-plane BD along Γ-X can be measured

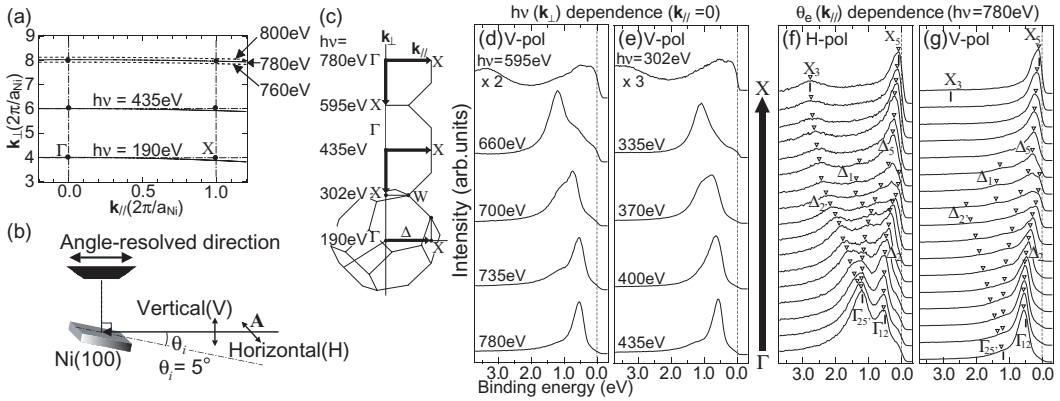

Fig. 1 – (a) $\boldsymbol{k}_\perp$ *vs.* $\boldsymbol{k}_\parallel$ for soft X-ray ARPES of Ni(100) for $h\nu = 190$, 435 and 780 eV photons by the experimental geometry used ((b)). Part (c) shows the 3D BZ of Ni(100) alongwith the probed sections. For $\boldsymbol{k}_\parallel = 0$ and $h\nu = 780$–595 eV (d) and 435–302 eV (e), nearly identical spectra in successive BZs, which are normalized by photon flux, verify the validity of the $\boldsymbol{k}_\perp$-points shown in (a) and (c). Soft X-ray ($h\nu = 780$ eV) ARPES of Ni(100) along Γ-X (Δ-line) with H- (f) and V-polarization (g), where each spectrum is integrated over 0.5°. Peak positions ($\bigtriangledown$) indicate BDs (Δ_2, Δ_5, Δ_1 and $\Delta_{2'}$).

by ARPES with 190, 435, and 780 eV photons. The probing depth or MFP is estimated to be about 5, 8, and 12 Å at $h\nu = 190$, 435, and 780 eV, respectively [9]. Thus, we can probe up to the third, fifth, and seventh layer of equivalent regions in the 3D BZ (figs. 1(a)-(c)).

ARPES with soft X-rays can also lead to indirect transitions caused by the phonon scattering [30]. However, recent ARPES studies with soft X-rays have shown that this can be avoided and the band dispersion can be measured by cooling the sample [31]. Therefore, the present ARPES experiments were performed at 50 K to minimize the influence of thermal diffuse scattering and hence maximize the direct transition component.

Results and discussion. – In figs. 1(f) and (g) we show the ARPES spectra of Ni(100) excited by 780 eV photons with H- and V-polarization, from Γ to X. The spectra show angular dependence in $\boldsymbol{k}$-space from Γ to X due to BDs, as marked with triangles. At the Γ-point in fig. 1(f), the two peaks correspond to the critical points $\Gamma_{25'}$ and Γ_{12} at 1.21 eV and 0.51 eV binding energy. Two bands disperse from $\Gamma_{25'}$ towards the X-point and a third band disperses from Γ_{12}, corresponding to $\Delta_{2'}$, Δ_5, and Δ_2 bands, respectively (fig. 1(f)). Features due to a fourth weak band (Δ_1) are also barely seen. These BDs are almost consistent with ARUPS results [10–15]. Especially, the energy positions at the high symmetry Γ- and X-point are very consistent with (spin-integrated) ARUPS results indicated by bars in fig. 1(f). Figure 1(g) (V-polarization) reproduces the energy positions of the critical points Γ_{12} and $X_{5\uparrow}$, with consistent BDs as in fig. 1(f) (H-polarization), but enhances the Δ_2 band relative to other bands [32]. The results indicate that soft X-ray ARPES can be surely used to obtain BDs of solids. However, there is one important discrepancy in the present data compared with ARUPS results. The Δ_2 band crosses the E_F in the present spectra and its energy position at the X-point, that is X_2, is evidently above E_F. This is in contrast with ARUPS studies [12,14] which show that the majority and minority bands of Δ_2 symmetry do not cross E_F, but remain below E_F all along the Δ-line.

As a check of the Δ_2 BD measured using $h\nu = 780$ eV, and if truly so, to investigate its deviation from ARUPS results, we measured BDs with $h\nu = 435$ and 190 eV. In order to

clearly see BDs, we plot band maps (BM) (second derivative of raw spectra after smoothing). Figures 2(a)-(c) show BMs made using the raw spectra shown in figs. 2(d)-(f) obtained with V-polarization using $h\nu = 780$, 435, and 190 eV, respectively. In fig. 2(a), the Δ_2 BD can be followed unambiguously and the E_F crossing is clearly observed (arrow mark), corresponding to the $\Delta_{2\downarrow}$ minority band. The $\Delta_{2\uparrow}$ majority BD also can be seen in fig. 2(a) but is clearer in figs. 2(b) and (c), with $X_{2\uparrow}$ located at 0.27 eV binding energy. The spectral intensity very close to the E_F crossing of $\Delta_{2\downarrow}$ (fig. 2(a), just next to the arrow mark), disperses to higher binding energy and is assigned to $\Delta_{5\downarrow}$. Additional confirmation comes from the 435 eV BM in fig. 2(b) which shows nearly identical BDs, but for a small change of the E_F crossing point in $\boldsymbol{k}$-space (arrow mark). The changed BD of the $\Delta_{2\downarrow}$ band with 435 eV photons (fig. 2(b)) results in overlapping the $\Delta_{5\downarrow}$ band at E_F, which are separated with 780 eV photons in fig. 2(a). The most important result is obtained with the $h\nu = 190$ eV BM shown in fig. 2(c). This BM shows well-resolved majority ($\Delta_{2\uparrow}$) and minority ($\Delta_{2\downarrow}$) bands. Probing just beyond the ARUPS regime changes BDs which are clearly intermediate to the bulk BDs (obtained with $h\nu = 435$ and 780 eV) and surface BDs obtained by ARUPS [10–15]. The $\Delta_{2\downarrow}$ band crosses E_F at 0.57(Γ-X) in fig. 2(a), at 0.62(Γ-X) in fig. 2(b), whereas it is 0.76(Γ-X) in fig. 2(c). The shift of the E_F crossing is also seen in the raw ARPES spectra (figs. 2(d)-(f)), which show clear E_F crossings with each photon energy (blue curves). The group velocity at E_F also changes systematically from 0.62 eVÅ (190 eV), to 0.82 eVÅ (435 eV) and 1.11 eVÅ (780 eV). Since the $\Delta_{2\downarrow}$ BD changes systematically, the results indicate that the Δ_2 bandwidth and the $(X_{2\uparrow} - X_{2\downarrow})$ ES are increased in the bulk compared to the ARUPS results. From ARUPS the ES is estimated to be 170 meV, an anomalously low ES measured only for the X_2-point on the surface [12,14,19].

We next check how the E_F crossing of $\Delta_{2\downarrow}$ is sensitive to the $\boldsymbol{k}_\perp$-point in the Ni band structure. The BMs with 800 eV and 760 eV photons (figs. 2(g) and (h)), which correspond to a $\approx \pm 10\%$ variation in $\boldsymbol{k}_\perp$ along Γ-X (see fig. 1(a)) as compared to data obtained with 780 eV photons (fig. 2(a)) show very similar BDs and also the E_F crossing of $\Delta_{2\downarrow}$ as in fig. 2(a). Therefore, the BD is insensitive to the $\boldsymbol{k}_\perp$ variations in the range of $\sim 0.1(\Gamma$-$X)$ for high energies and the change in E_F crossing is not due to a change of the $\boldsymbol{k}_\perp$-point.

Since, at any photon energy, the experiments actually measure an integral of the intensity, weighted by an exponential factor for the MFP, we try to extract the bulk BD from ARPES with 780 eV photons. The spectra with 780 eV photons is estimated to roughly contain about 50% contribution from the top 4-5 layers, which is the probing depth at $h\nu = 435$ eV. The ARPES spectra with 780 eV photons are subtracted by the 435 eV spectra weighted by the exponential factor (0.52) and assuming atomic cross-sections. The result is shown in fig. 2(i) and confirms that the BDs seen for bulk Ni are similar to the data of fig. 2(a). In particular, the separate BDs are clearer at the X-point. The data thus prove that the $\Delta_{2\downarrow}$ BD is different in the bulk compared to surface-sensitive ARUPS studies (overlaid as green line).

Thus, the reduced probing depth measurements indicate bulk in-plane BD of the $\Delta_{2\downarrow}$ band systematically connects to the ARUPS results [10–15]. The $\Delta_{2\downarrow}$ band which is pinned just below E_F at the X-point ($X_{2\downarrow}$) in surface-sensitive ARUPS, crosses E_F in bulk-sensitive ARPES with $X_{2\downarrow}$ lying above E_F. This leads to an additional minority spin $X_{2\downarrow}$ hole pocket. There exists an early spin-polarized study by Kisker *et al.* [33] showing that the $X_{2\downarrow}$ state lies above E_F although later studies have concluded it lies below E_F. In view of the present results, the larger MFP used but at very low energy (4–6 eV) by Kisker *et al.* [33] reflects the bulk BS [4]. While de Haas-van Alphen measurements also showed only the $X_{5\downarrow}$ hole pocket along Γ to X [34], magneto-crystalline anisotropy measurements [35] indicated evidence for the additional $X_{2\downarrow}$ hole pocket.

The layer-dependent BD is coupled to the widening of the Δ_2 bandwidth observed in ARPES using high $h\nu$, suggesting weaker electron-electron correlations in the bulk. The-

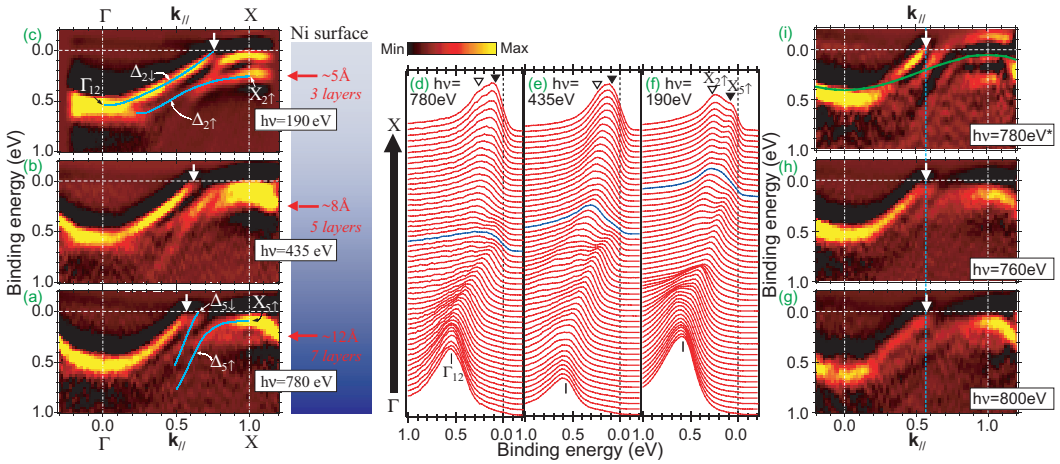

Fig. 2 – Band maps of Ni(100) along Γ-X (Δ-line) using (a) $h\nu = 780$ eV, (b) 435 eV and (c) 190 eV, with V-polarization. Arrows indicate $\boldsymbol{k}$-points, where the $\Delta_{2\downarrow}$ band crosses $E_{\rm F}$. The blue lines show the observed band dispersions. The raw ARPES spectra with (d) 780 eV (e) 435 eV and (f) 190 eV were used to obtain BMs of (a)-(c). The spectra showing $E_{\rm F}$ crossings are plotted with blue curves in (d)-(f). (g) and (h) show the BMs with 800 eV and 760 eV photons. (i) is obtained as $I(780\,\text{eV}^*) = I(780) - 0.52I(435)$ (I: intensity weighted by atomic cross-sections after being normalized by photon flux). The green line shows the $\Delta_{2\downarrow}$ band dispersion summarized from low-energy ARUPS studies and inverse-photoemission studies [10–19], which are reproduced by GWA + DMFT [25] calculation.

oretical calculations which include Coulomb correlations show that $X_{2\downarrow}$ is located below $E_{\rm F}$ [14, 19, 23–25] in contrast to s-LDA calculations [22] and the 6 eV satellite is also reproduced [23–25]. Hence, we checked for variations of ARPES spectra in the 6 eV satellite region as a function of $h\nu$ (figs. 3(a) and (b)). The ARPES spectra show the Δ_1 band dispersing

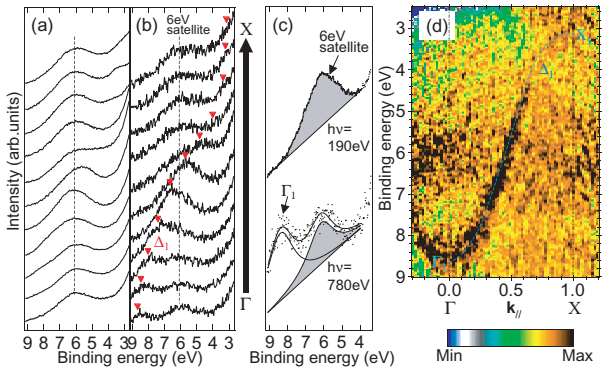

Fig. 3 – ARPES spectra with $h\nu = 190$ (a) and 780 eV (b), for the 6 eV satellite from Γ to X, normalized for the area under the curve of the entire valence band. Triangles in (b) indicate Δ_1 BD obtained from fig. 3(d). (c) A blow-up of the 6 eV satellite feature at the Γ-point for the same normalization. Curve fits (solid curves) indicate a reduction of $\sim 20 \pm 4\%$ in the 6 eV satellite intensity for $h\nu = 780$ eV (shaded area), but no weakening of the correlation energy, consistent with its localized nature. (d) The BM between 2.5 and 9.0 eV binding energy showing Δ_1 BD (broken curve).

across and overlapping the 6 eV satellite between Γ to X, as expected from s-LDA calculations [22] and ARUPS studies [10–15]. Even though the $4sp$ character Δ_1 band crossing makes quantification very difficult, an attempt to do so with the Γ-point spectra (fig. 3(c)), where the Δ_1 band is separated, shows a reduction of $\sim 20 \pm 4\%$ in the 6 eV satellite intensity on increasing $h\nu$ from 190 to 780 eV. This reduction in intensity is small and not conclusive but suggestive of reduced correlations in the bulk [16–18, 23], consistent with the layer-dependent change of the $\Delta_{2\downarrow}$ band dispersion in fig. 2. Also, since the electron correlation in nickel leads to a reduced ES compared to the s-LDA calculation [19, 25], the reduced correlation is consistent with the enhancement of the ES observed at X_2. Since the 6 eV satellite feature is still observed with 780 eV photons as in angle-integrated X-PES studies [16], it shows that ARPES is necessary to check for the bulk to surface changes in the valence BS. In fig. 3(d), we plot a BM for 2.5 to 9.0 eV binding energy and $h\nu = 780$ eV, where the Δ_1 BD is clearly seen, consistent with ARUPS results. We have also confirmed that the Δ_1 BD is similar to that obtained by applying the sum rule as discussed in ref. [36].

Another important point to note is that the Δ_5 and $\Delta_{2'}$ (fig. 1(f)) BDs do not change with $h\nu$ *i.e.* as a function of probing depth. Since the Δ_5 and $\Delta_{2'}$ bands originate in t_{2g}-type states, they are not modified by electron correlations like the e_g-derived states [23]. Even between the e_g-derived states, the Δ_2 band ($d_{x^2-y^2}$) possibly shows more layer-dependent correlation than the Δ_1 band ($d_{z^2-r^2}$) since the ($d_{x^2-y^2}$) orbital extends outwards along the surface normal direction (100). This suggests similarity to recent results showing varying correlations between the t_{2g}-orbitals of (d_{xy}), (d_{xz}), and (d_{yz}) symmetry for correlated oxides [5].

Conclusion. – In conclusion, tunable soft X-ray polarization-dependent ARPES makes it possible to resolve the changes in BDs with specified symmetry and layers. We observe layer-dependent $\Delta_{2\downarrow}$ band dispersion, which leads to an additional minority spin $X_{2\downarrow}$ hole pocket. However, the Δ_5 and $\Delta_{2'}$ (t_{2g})-symmetry bands are not affected by the existence of the surface. Thus, the observed bulk *vs.* surface difference in the behavior of the electronic states depends on the band symmetry. The results show layer-dependent BD changes, suggesting correlation effects and ES being coupled to changes in the probing depth, and the importance of Coulomb correlations in theoretical calculations for the surface electronic BS. Soft X-ray ARPES is thus shown to be a very important tool to study layer-dependent BD of 3D solids.

* * *

We thank Drs H. OHASHI, Y. TAMENORI, T. ITO, and P. A. RAYJADA for help with experiments and Profs. A. FUJIMORI, T. YOKOYA, A. KOTANI, M. TAGUCHI, M. USUDA, T. JO, and Dr K. HORIBA for valuable discussions.

REFERENCES

[1] SEGOVIA P., PURDIE D., HENGSBERGER M. and BAER Y., *Nature*, **402** (1999) 504.
[2] VALLA T. *et al.*, *Nature*, **417** (2002) 627.
[3] LANZARA A. *et al.*, *Nature*, **412** (2001) 510; KAMINSKI A. *et al.*, *Nature*, **416** (2002) 610; YUSOF Z. M. *et al.*, *Phys. Rev. Lett.*, **88** (2002) 167006.
[4] PLUMMER E. W. and EBERHARDT W., *Adv. Chem. Phys.*, **49** (1982) 533.
[5] LIEBSCH A., *Phys. Rev. Lett.*, **90** (2003) 096401; SCHWIEGER S., POTTHOFF M. and NOLTING W., *Phys. Rev. B*, **67** (2003) 165408.
[6] RADER O. *et al.*, *Europhys. Lett.*, **39** (1997) 429.
[7] SEKIYAMA A. *et al.*, *Nature*, **403** (2000) 396.

[8] Maiti K., Mahadevan P. and Sarma D. D., *Phys. Rev. Lett.*, **80** (1998) 2885; Mo S.-K. *et al.*, *Phys. Rev. Lett.*, **90** (2003) 186403.

[9] Tanuma S., Powell C. J. and Penn D. R., *Surf. Interface Anal.*, **11** (1988) 57.

[10] Himpsel F. J., Knapp J. A. and Eastman D. E., *Phys. Rev. B*, **19** (1979) 2919.

[11] Eberhardt W. and Plummer E. W., *Phys. Rev. B*, **21** (1980) 3245.

[12] Heimann P., Himpsel F. J. and Eastman D. E., *Solid State Commun.*, **39** (1981) 219.

[13] Mårtensson H. and Nilsson P. O., *Phys. Rev. B*, **30** (1984) 3047.

[14] Bünemann J., Gebhard F., Ohm T., Umstätter R., Weiser S., Weber W., Claessen R., Ehm D., Harasawa A., Kakizaki A., Kimura A., Nicolay G., Shin S. and Strocov V. N., *Europhys. Lett.*, **61** (2003) 667.

[15] Kakizaki A. *et al.*, *Phys. Rev. Lett.*, **72** (1994) 2781; Greber T., Kreutz T. J. and Osterwalder J., *Phys. Rev. Lett.*, **79** (1997) 4465.

[16] Hüfner S. *et al.*, *Solid State Commun.*, **11** (1972) 323.

[17] Guillot C. *et al.*, *Phys. Rev. Lett.*, **39** (1977) 1632.

[18] Kinoshita T. *et al.*, *Phys. Rev. B*, **47** (1993) 6787; Sinkovic B. *et al.*, *Phys. Rev. Lett.*, **79** (1997) 3510.

[19] Donath M., *Surf. Sci. Rep.*, **20** (1994) 251.

[20] Slater J. C., *Phys. Rev.*, **49** (1936) 537.

[21] Stoner E. C., *Proc. R. Soc. London, Ser. A*, **165** (1938) 372.

[22] Wang C. S. and Callaway J., *Phys. Rev. B*, **15** (1977) 298.

[23] Liebsch A., *Phys. Rev. Lett.*, **43** (1979) 1431.

[24] Lichtenstein A. I., Katsnelson M. I. and Kotliar G., *Phys. Rev. Lett.*, **87** (2001) 067205.

[25] Biermann S., Aryasetiawan F. and Georges A., *Phys. Rev. Lett.*, **90** (2003) 086402.

[26] Ohashi H. *et al.*, *Nucl. Instrum. Methods A*, **467-468** (2001) 529.

[27] Tanaka T. and Kitamura H., *J. Synchrotron Radiat.*, **3** (1996) 47.

[28] It is also possible to measure $\boldsymbol{k}_{\parallel}$ band dispersions in the constant final state (CFS) mode without $\boldsymbol{k}_{\perp}$ variation compared to the energy distribution curve (EDC) mode described, even with ARUPS, see, *e.g.*, Cardona M. and Ley L. (Editors), *Photoemission in Solids*, Vol. **I** (Springer-Verlag, Berlin) 1978, p. 261.

[29] This is understood from the measured spectra which show constant shifts in $\boldsymbol{k}_{\parallel}$ by $0.22(\Gamma\text{-}X)$, while the $\boldsymbol{k}_{\perp}$ negligibly shifts, for 780 eV. Similarly, for $h\nu = 435$ eV and 190 eV, constant $\boldsymbol{k}_{\parallel}$ shifts of $0.12(\Gamma\text{-}X)$ and $0.05(\Gamma\text{-}X)$ were determined. The shift of $\boldsymbol{k}$ is identified from the accurate determination of the high symmetry points Γ and X.

[30] Shevchik N. J., *Phys. Rev. B*, **16** (1977) 3428; **20** (1979) 3020; Hussain Z., Kono S., Peterson L. G., Fadley C. S. and Wagner L. F., *Phys. Rev. B*, **23** (1981) 724.

[31] Hofmann Ph. *et al.*, *Phys. Rev. B*, **66** (2002) 245422; Nielsen M. B., Li Z., Lizzit S., Goldoni A. and Hofmann Ph., *J. Phys. Condens. Matter*, **15** (2003) 6919.

[32] In figs. 1(d) and (e), the Δ_1 band should be mainly observed due to dipole selection rules and the intensity decrease at the X-point seen in the figure is caused by the Δ_1 band moving above E_{F}, as also expected from ARUPS. In figs. 1(f) and (g), on the other hand, bands with all symmetries along Δ can be observed because of the measurement of the in-plane band dispersion, and the relative intensity of each band is governed by matrix elements. The differences in spectra are also attributed to the different volumes sampled with the different photon energies used.

[33] Kisker E., Gudat W., Kuhlmann E., Clauberg R. and Campagna M., *Phys. Rev. Lett.*, **45** (1980) 2053.

[34] Tsui D. C. and Stark R. W., *Phys. Rev. Lett.*, **17** (1966) 871.

[35] Gersdorf R., *Phys. Rev. Lett.*, **40** (1978) 344.

[36] Freund H.-J., Eberhardt W., Heskett D. and Plummer E. W., *Phys. Rev. Lett.*, **50** (1983) 768.